Article

The Theory of Electron Transfer Reactions: What May Be Missing?

David W. Small, Dmitry V. Matyushov, and Gregory A. Voth

J. Am. Chem. Soc., **2003**, 125 (24), 7470-7478• DOI: 10.1021/ja029595j • Publication Date (Web): 21 May 2003

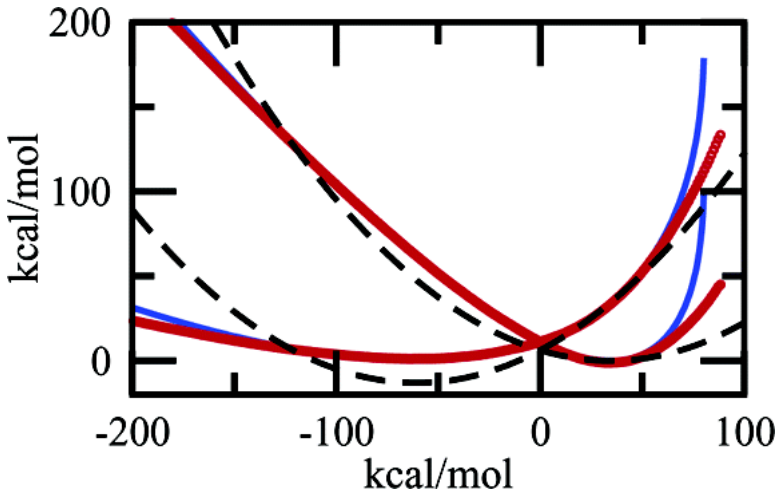

More About This Article

Additional resources and features associated with this article are available within the HTML version:

- Supporting Information
- Links to the 12 articles that cite this article, as of the time of this article download
- Access to high resolution figures
- Links to articles and content related to this article
- Copyright permission to reproduce figures and/or text from this article

View the Full Text HTML

J|A|C|S
ARTICLES
Published on Web 05/21/2003

The Theory of Electron Transfer Reactions: What May Be Missing?

David W. Small,[†] Dmitry V. Matyushov,[‡] and Gregory A. Voth*,[†]

Contribution from the Department of Chemistry and Henry Eyring Center for Theoretical Chemistry, 315 South 1400 East Rm 2020, University of Utah, Salt Lake City, Utah 84112-0850, and Department of Chemistry and Biochemistry, Arizona State University, P.O. Box 871604, Tempe, Arizona 85287-1604

Received December 6, 2002; E-mail: voth@chem.utah.edu

Abstract: Molecular dynamics simulations are presented for condensed-phase electron transfer (ET) systems where the electronic polarizability of both the solvent and the solute is incorporated. The solute polarizability is allowed to change with electronic transition. The results display notable deviation from the standard free energy parabolas of traditional ET theories. A new three-parameter ET model is applied, and the theory is shown to accurately model the free energy surfaces. This paper presents conclusive evidence that the traditional theory for the free energy barrier of ET reactions requires modification.

I. Introduction

The study of condensed-phase electron transfer (ET) reactions is essential in chemistry, biology, physics,[1] and in the emerging field of molecular electronics.[2] A considerable amount of work has been invested in the development of ET theory, a very notable contribution to which is by Marcus.[1a,c,3] Through both theoretical and experimental explorations, this theory has been applied to a multitude of systems.[1,3,4] The Marcus formulation connects ET activation with fluctuations of the electronic levels of the donor and acceptor linearly coupled to a solvent thermal bath characterized by Gaussian statistics. This consideration leads to the picture of intersecting parabolas in which the ET activated state is achieved at the crossing point. The curvatures of the two parabolas are equal as a consequence of the Gaussian statistics of the energy fluctuations.[5]

The issue of whether the free energy surfaces are parabolic has been actively discussed in both experimental and theoretical literature in recent decades. Experimentally, the problem is addressed by measuring the energy gap law, that is, the dependence of the activation barrier on the ET driving force (the free energy gap between the minima of ET surfaces).[6−10] The results of experimental studies can be summarized as follows: (1) The energy gap dependence goes through a maximum, in excellent agreement with the prediction of the Marcus theory. (2) The bell-shaped dependence is, however, asymmetric with usually a steeper slope in the normal region of ET. One explanation proposed for this effect is preferential transitions to excited vibrational states in the ET inverted region. (3) The energy gap law switches from a bell-shaped form in the region close to the maximum to a linear dependence on the driving force far away from the maximum point as is usually explained within vibronic models.[4b,11]

[†] University of Utah.
[‡] Arizona State University.

(1) (a) Marcus, R. A.; Sutin, N. *Biochim. Biophys. Acta* **1985**, *811*, 265. (b) *Electron Transfer in Inorganic, Organic, and Biological Systems*; Bolton, J. R., Mataga, N., McLendon, G., Eds.; *Advances in Chemistry Ser.*; American Chemical Society: Washington, DC, 1991; Vol. 228. (c) Marcus, R. A. *Rev. Mod. Phys.* **1993**, *65*, 599. (d) Barbara, P. F.; Meyer, T. J.; Ratner, M. A. *J. Phys. Chem.* **1996**, *100*, 13148. (e) Warshel, A.; Parson, W. W. *Annu. Rev. Phys. Chem.* **1991**, *42*, 279.
(2) (a) Alivisatos, A. P.; Barbara, P. F.; Castleman, A. W.; Chang, J.; Dixon, D. A.; Klein, M. L.; McLendon, G. L.; Miller, J. S.; Ratner, M. A.; Rossky, P. J.; Stupp, S. I.; Thompson, M. E. *Adv. Mater.* **1998**, *10*, 1297. (b) Ratner, M. A.; Jortner, J. In *Molecular Electronics: Some Directions*; Ratner, M. A., Jortner, J., Eds.; IUPAC, 1997.
(3) (a) Marcus, R. A. *J. Chem. Phys.* **1956**, *24*, 966. (b) Marcus, R. A. *J. Chem. Phys.* **1956**, *24*, 979. (c) Marcus, R. A. *Can. J. Chem.* **1959**, *37*, 155. (d) Marcus, R. A. *J. Chem. Phys.* **1957**, *26*, 867. (e) Marcus, R. A. *J. Chem. Phys.* **1957**, *26*, 872. (f) Marcus, R. A. *Discuss. Faraday Soc.* **1960**, *29*, 21. (g) Marcus, R. A. *J. Phys. Chem.* **1963**, *67*, 853. (h) Marcus, R. A. *Annu. Rev. Phys. Chem.* **1964**, *15*, 155. (i) Marcus, R. A. *J. Chem. Phys.* **1965**, *43*, 679. (j) Marcus, R. A. *Electrochim. Acta* **1968**, *13*, 995.
(4) (a) See review articles in: *Adv. Chem. Phys.* **1999**, *106*−*107*. (b) Chen, P.; Meyer, T. J. *Chem. Rev.* **1998**, *98*, 1439. (c) Demadis, K. D.; Hartshorn, C. M.; Meyer, T. J. *Chem. Rev.* **2001**, *101*, 2655. (d) Barzikin, A. V.; Frantsuzov, P. A.; Seki, K.; Tachiya, M. *Adv. Chem. Phys.* **2002**, *123*, 511.
(5) (a) Hwang, J.-K.; Warshel, A. *J. Am. Chem. Soc.* **1987**, *109*, 715. (b) Tachiya, M. *Chem. Phys. Lett.* **1989**, *159*, 505. (c) Tachiya, M. *J. Phys. Chem.* **1989**, *93*, 7050.
(6) (a) Miller, J. R.; Calcaterra, L. T.; Closs, G. L. *J. Am. Chem. Soc.* **1984**, *106*, 3047. (b) Wasielewski, M. R.; Niemczyk, M. P.; Svec, W. A.; Pewitt, E. B. *J. Am. Chem. Soc.* **1985**, *107*, 1080.
(7) (a) Kakitani, T.; Mataga, N. *J. Phys. Chem.* **1985**, *89*, 8. (b) Kakitani, T.; Mataga, N. *J. Phys. Chem.* **1985**, *89*, 4752. (c) Asahi, T.; Ohkohchi, M.; Matsusaka, R.; Mataga, N.; Zhang, R. P.; Osuka, A.; Maruyama, K. *J. Am. Chem. Soc.* **1993**, *115*, 5665. (d) Kakitani, T.; Matsuda, N.; Yoshimori, A.; Mataga, N. *Prog. React. Kinet.* **1995**, *20*, 347. (e) Yoshimori, A.; Mataga, N. *J. Phys. Soc. Jpn.* **1992**, *61*, 2577. (f) Mataga, N.; Chosrowjan, H.; Taniguchi, S.; Shibata, Y.; Yoshida, N.; Osuka, A.; Kikuzawa, T.; Okada, T. *J. Phys. Chem. A* **2002**, *106*, 12191.
(8) (a) Kober, E. M.; Caspar, J. V.; Lumpkin, R. S.; Meyer, T. J. *J. Phys. Chem.* **1986**, *90*, 3722. (b) Worl, L. A.; Duesing, R.; Chen, P.; Ciana, L. D.; Meyer, T. J. *J. Chem. Soc., Dalton Trans.* **1991**, 849. (c) Claude, J. D.; Meyer, T. J. *J. Phys. Chem.* **1995**, *99*, 51.
(9) (a) Heitele, H.; Pöllinger, F.; Häberle, T.; Michel-Beyerle, M. E.; Staab, H. A. *J. Phys. Chem.* **1994**, *98*, 7402. (b) Cortés, J.; Heitele, H.; Jortner, J. *J. Phys. Chem.* **1994**, *98*, 2527. (c) Bixon, M.; Jortner, J.; Cortes, J.; Heitele, H.; Michel-Beyerle, M. E. *J. Phys. Chem.* **1994**, *98*, 7289.
(10) (a) Asahi, T.; Mataga, N. *J. Phys. Chem.* **1989**, *93*, 6575. (b) Segawa, H.; Takehara, C.; Honda, K.; Shimidzu, T.; Asahi, T.; Mataga, N. *J. Phys. Chem.* **1992**, *96*, 503. (c) Benniston, A. C.; Harriman, A.; Philp, D.; Stoddart, J. F. *J. Am. Chem. Soc.* **1993**, *115*, 5298. (d) Hirsch, T.; Port, H.; Wolf, H. C.; Miehlich, B.; Effenberger, F. *J. Phys. Chem. B* **1997**, *101*, 4525. (e) Tétreault, N.; Muthyala, R. S.; Liu, R. S. H.; Steer, R. P. *J. Phys. Chem. A* **1999**, *103*, 2524.

10.1021/ja029595j CCC: $25.00

None of the above observations contradict the Marcus theory, requiring only an accounting for the quantum skeletal vibrations within the donor−acceptor complex in addition to the classical solvent fluctuations.[11f] There are, however, two types of experiments which call for a closer scrutiny of the basic assumptions embodied in the Marcus picture. The first observation, first noticed by Mataga and co-workers,[7] indicates a substantial asymmetry of energy gap laws between charge-separation (CS) and charge-recombination (CR) reactions. Indeed, the combined effect of classical solvent fluctuations and quantum skeletal vibrations does create Franck−Condon factors that are asymmetric relative to their maxima. However, the combination of the Gaussian statistics of nuclear fluctuations[3] with the Poisson statistics of quantum skeletal vibrations[11] predicts that the absorption and emission bands should be related by mirror symmetry,[11] thus resulting in identical energy gap laws for CS and CR reactions. In fact, symmetry between absorption and emission lines is rarely observed in steady-state optical experiments.[12] (For more discussion of this issue, see the first paragraph of section VI.) The second category of experiments is in the time-resolved domain. Recent observations of the time-resolved dynamics of absorption and emission optical bands indicate substantial temporal changes in the inhomogeneous optical width,[13] in contrast to the prediction of constant width in the Marcus picture. The origin of both static (energy gap law) and dynamic (time-resolved spectroscopy) effects may be understood either through the solvent effect[13d] or through the change of normal-mode frequencies of the donor−acceptor complex.[13h,14] It remains a significant experimental challenge to separate these two effects.[15]

Theoretically, the problem of the shape of the ET free energy surfaces has been addressed predominantly by estimating possible effects of nonlinear solvation on the thermodynamics[16,17] and dynamics[16b,18] of charge transfer. Nonlinear solvation may cause the Marcus picture to break down via two possible scenarios: (1) due to non-Gaussian statistics of the fluctuations of solvent modes coupled to electronic levels of the donor and acceptor, and (2) through a generally nonlinear dependence of the solute−solvent interaction potential on molecular solvent coordinates. Computer simulations have been employed to calculate the shapes of ET free energy surfaces.[16,17] The common setup in simulations modeling ET includes a donor−acceptor complex, immersed in a molecular solvent, with a charge distribution changing diabatically with electronic transitions. Certain deviations from parabolic free energy surfaces have been observed in systems with strong solute−solvent coupling by direct calculations of the free energy surfaces[16b−d,17b−d] and from the dynamic response.[18b,d] However, these nonlinear solvation effects are commonly much smaller than distortions of the equal-curvature parabolas seen in experiment.[7,13] The consensus that seems to arise in the field is that nonlinear solvation is not capable of producing a significant effect on the free energy surfaces of realistic systems, which are often composed of bulky organic molecules dissolved in dense molecular solvents.

Something that is lacking in most theoretical models of ET is a recognition of the fact that not only does the distribution of the electronic density change with electronic transitions, but also does the self-energy of the electronic subsystem of the donor−acceptor complex. This change in self-energy arises from the difference in the polarization of the electronic cloud of the donor−acceptor complex by the solvent in the reactant and product states. It is responsible for the ability of the solute electronic density to readjust to external perturbations generated by the nuclear subsystem. Physically, this effect results in a difference in the linear and higher order polarizabilities of the two ET states and/or a difference in the extent of electronic delocalization between the donor and acceptor units. Both effects lead to a significant distortion of the free energy surfaces that far exceeds the nonlinear solvation effect.[19−22] The goal of this work is to study nonlinear distortions of the ET free energy surfaces arising from the solute electronic effect, that is, the effect due to a varying solute electronic polarizability. The explicit computer simulations carried out in this study indicate that the Marcus picture of parabolic surfaces can seriously break down in realistic systems when the electronic polarizability is allowed to vary with the progress of the ET reaction from the reactant to product states.

II. Traditional Electron Transfer Theory

Modern ET reaction theory dates back to the 1950s, the most important developments commencing with Marcus' seminal 1956 papers.[3a,b] Beginning with these articles, and extending through work in the following two decades, Marcus developed the following elegant picture.

(11) (a) Huang, K.; Rhys, A. *Proc. R. Soc.* **1950**, *204A*, 406. (b) Kubo, R.; Toyozawa, Y. *Prog. Theor. Phys.* **1955**, *13*, 160. (c) Lax, M. *J. Chem. Phys.* **1955**, *20*, 1752. (d) Englman, R.; Jortner, J. *Mol. Phys.* **1970**, *18*, 145. (e) Kestner, N. R.; Logan, J.; Jortner, J. *J. Phys. Chem.* **1974**, *21*, 2148. (f) Bixon, M.; Jortner, J. *Adv. Chem. Phys.* **1999**, *106*, 35.

(12) (a) Horng, M. L.; Gardecki, J. A.; Papazyan, A.; Maroncelli, M. *J. Phys. Chem.* **1995**, *99*, 17311. (b) Cao, X.; McHale, J. L. *J. Chem. Phys.* **1998**, *109*, 1901. (c) Boldrini, B.; Cavalli, E.; Painelli, A.; Terenziani, F. *J. Phys. Chem. A* **2002**, *106*, 6286.

(13) (a) Tominaga, K.; Walker, G. C.; Jarzeba, W.; Barbara, P. F. *J. Phys. Chem.* **1991**, *95*, 10475. (b) Bingemann, D.; Ernsting, N. P. *J. Chem. Phys.* **1992**, *102*, 2691. (c) Gustavsson, T.; Baldacchino, G.; Mialocq, J.-C.; Pommeret, S. *Chem. Phys. Lett.* **1995**, *236*, 587. (d) van der Meulen, P.; Jonkman, A. M.; Glasbeek, M. *J. Phys. Chem. A* **1998**, *102*, 1906. (e) Nishiyama, K.; Okada, T. *J. Phys. Chem. A* **1998**, *102*, 9729. (f) Richert, R. *J. Chem. Phys.* **2001**, *114*, 7471. (g) Kovalenko, S. A.; Ruthmann, J.; Ernsting, N. P. *Chem. Phys. Lett.* **1997**, *271*, 40. (h) Kovalenko, S. A.; Eilers-König, N.; Senyushkina, T. A.; Ernsting, N. P. *J. Phys. Chem. A* **2001**, *105*, 4834. (i) Sluch, M. I.; Godt, A.; Bunz, U. H. F.; Berg, M. A. *J. Am. Chem. Soc.* **2001**, *123*, 6447.

(14) (a) Mebel, A. M.; Hayashi, M.; Liang, K. K.; Lin, S. H. *J. Phys. Chem. B* **1999**, *103*, 10674. (b) Sando, G. M.; Spears, K. G.; Hupp, J. T.; Ruhoff, P. T. *J. Phys. Chem. A* **2001**, *105*, 5317.

(15) Myers Kelley, A. *J. Phys. Chem. A* **1999**, *103*, 6891.

(16) (a) King, G.; Warshel, A. *J. Chem. Phys.* **1990**, *93*, 8682. (b) Carter, E. A.; Hynes, J. T. *J. Phys. Chem.* **1989**, *93*, 2184. (c) Ichiye, T. *J. Chem. Phys.* **1996**, *104*, 7561. (d) Yelle, R. B.; Ichiye, T. *J. Phys. Chem. B* **1997**, *101*, 4127.

(17) (a) Kuharski, R. A.; Bader, J. S.; Chandler, D.; Sprik, M.; Klein, M. L. *J. Chem. Phys.* **1988**, *89*, 3248. (b) Straus, J. B.; Voth, G. A. *J. Phys. Chem.* **1993**, *97*, 7388. (c) Straus, J. B.; Calhoun, A.; Voth, G. A. *J. Chem. Phys.* **1995**, *102*, 529. (d) Calhoun, A.; Voth, G. A. *J. Phys. Chem. B* **1998**, *102*, 8563.

(18) (a) Bader, J. S.; Chandler, D. *Chem. Phys. Lett.* **1989**, *157*, 501. (b) Ladanyi, B. M.; Skaf, M. S. *Annu. Rev. Phys. Chem.* **1993**, *44*, 335. (c) Kumar, P. V.; Maroncelli, M. *J. Chem. Phys.* **1995**, *103*, 3038. (d) Geissler, P. L.; Chandler, D. *J. Chem. Phys.* **2000**, *113*, 9759. (e) Nishiyama, K.; Hirata, F.; Okada, T. *J. Mol. Struct.* **2001**, *565*−*566*, 31. (f) Marchi, M.; Gehlen, J. N.; Chandler, D.; Newton, M. *J. Am. Chem. Soc.* **1993**, *115*, 4178.

(19) Matyushov, D. V.; Voth, G. A. *J. Phys. Chem. A* **1999**, *103*, 10981.

(20) (a) Matyushov, D. V.; Voth, G. A. *J. Phys. Chem. A* **2000**, *104*, 6470. (b) Matyushov, D. V.; Voth, G. A. *J. Phys. Chem. A* **2000**, *104*, 6485. (c) Matyushov, D. V.; Newton, M. D. *J. Phys. Chem. A* **2001**, *105*, 8516. (d) Matyushov, D. V.; Voth, G. A. In *Rev. Comput. Chem.*; Lipkowitz, K. B., Boyd, D. B., Eds.; Wiley-VCH: Hoboken, New Jersey, 2002; Vol. 18.

(21) (a) Bursulaya, B. D.; Zichi, D. A.; Kim, H. J. *J. Phys. Chem.* **1995**, *99*, 10069. (b) Bursulaya, B. D.; Zichi, D. A.; Kim, H. J. *J. Phys. Chem.* **1996**, *100*, 1392. (c) Bursulaya, B. D.; Kim, H. J. *J. Phys. Chem. B* **1997**, *101*, 10994. (d) Ando, K. *J. Chem. Phys.* **1997**, *107*, 4585.

(22) (a) Painelli, A.; Terenziani, F. *J. Phys. Chem. A* **2000**, *104*, 11041. (b) Terenziani, F.; Painelli, A.; Comoretto, D. *J. Phys. Chem. A* **2000**, *104*, 11049.

An ET reaction is, by definition, characterized by a change in the electron configuration of the reacting species. According to the Franck−Condon principle, this change occurs fast enough that the nuclei are effectively frozen during the transfer. Hence, the surrounding solvent molecules are suddenly in an unstable configuration, and they must reorient to find equilibrium with the new solute characteristics. Additionally, the electronic transition is accompanied by vibronic transitions that also lead to internal energy conversion after the transfer. Marcus termed the collective free energy for these processes as the reorganization energy, λ.[3a−e]

If an electronic transition occurs while the ET complex is in an equilibrium state (an endothermic process), energy must be provided, through, for example, the absorption of light. In the absence of photoexcitation, the transition is made possible through fluctuations in the surrounding solvent molecules. For a successful ET reaction, a nonequilibrium solvent configuration is reached at the classical transition state such that the potential energies of the reactant and product systems are equal for the current nuclear coordinates, and a zero energy Franck−Condon transition occurs.[3f] Here, the solvent provides the driving force for the reaction.

If a molecule undergoes an electronic transition through photoexcitation, the subsequent relaxation can be observed spectroscopically with the Stokes shift,[23] which is the difference between the maximum absorption and fluorescent emission energies

$$\lambda = \frac{\hbar\omega_1 - \hbar\omega_2}{2} = \frac{\hbar\Delta\omega_{st}}{2} \tag{1}$$

The validity of this relationship relies on the linear response approximation utilized by Marcus, which predicts that a change in the charge of the reacting species will result in a linearly proportional change in the dielectric polarization of the solvent medium.[3h] Under these conditions, the energies of reorganization after a transition from either reactant to product or product to reactant are the same. Using the same argument, one also easily finds the reaction free energy ΔF spectroscopically, through the mean energy of the absorption and emission maxima[23b]

$$\Delta F = \frac{\hbar\omega_1 + \hbar\omega_2}{2} = \hbar\omega_m \tag{2}$$

These linear response consequences may be more easily understood from diagrams depicting the free energies of such electronic transitions, as in Figure 1.

A hallmark of Marcus theory is that the activation free energy of an ET reaction, $\Delta F^{\ddagger}$, was found to be related to λ and ΔF by a simple parabolic expression[3h,k]

$$\Delta F^{\ddagger} = \frac{\lambda}{4}\left(1 + \frac{\Delta F}{\lambda}\right)^2 \tag{3}$$

The activation barrier is the crossing point of the two ET free energy surfaces plotted against a reaction coordinate representative of the charge transfer from the donor to the acceptor. Because the eigenvalues of the reactant and product electronic states become equal at the transition state, the gap, X, between

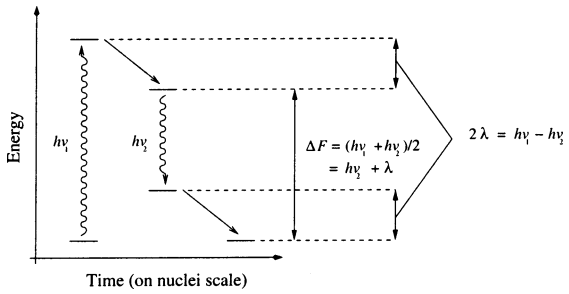

Figure 1. Simplified diagram depicting the dynamics of a photoinduced electron transfer reaction. The vertical transitions take place instantaneously on the nuclear time scale (Franck−Condon). The Marcus linear response approximation relates the Stokes shift and mean transition energy to the ET parameters.

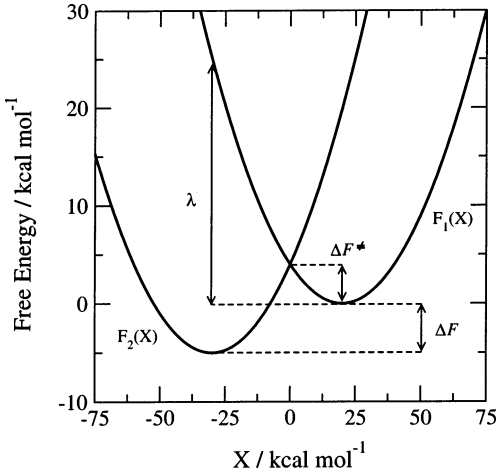

Figure 2. Example of Marcus theory free energy surfaces calculated from eqs 5 and 6. For these curves, the input parameter values are $\lambda = 25$ kcal mol^{-1} and $\Delta F = -5$ kcal mol^{-1}. Note the equal curvatures of the parabolas.

diabatic electronic energies at an instantaneous nuclear configuration provides a useful reaction coordinate:[3h,k,24]

$$X = E_2 - E_1 = \Delta E \tag{4}$$

where the subscripts 1 and 2 denote the initial and final ET solute energy states, respectively. The free energy invested in obtaining a particular energy gap X defines the ET free energies (with the $F_1(X)$ minimum set at 0):[3k,23b]

$$F_1(X) = \frac{(X - \lambda - \Delta F)^2}{4\lambda} \tag{5}$$

$$F_2(X) = \frac{(X + \lambda - \Delta F)^2}{4\lambda} + \Delta F \tag{6}$$

The crossing point of the two resulting surfaces corresponds to the activation free energy of the ET reaction, $\Delta F^{\ddagger}$ (eq 3), the vertical distance along one surface from one minimum to the other minimum is the reorganization energy, λ, and the vertical separation between the curve minima is the reaction free energy, ΔF. The horizontal distance between the minima is 2λ, and the curvature of each parabola is $(2\lambda)^{-1}$. These features are shown with two example free energy surfaces in Figure 2.

(23) (a) Marcus, R. A. *J. Chem. Phys.* **1963**, *38*, 1858. (b) Marcus, R. A. *J. Phys. Chem.* **1989**, *93*, 3078.

(24) Warshel, A. *J. Phys. Chem.* **1982**, *86*, 2218.

The true diabatic free energy surface, free from approximation, can be calculated from the following expression:[24]

$$F_i(X) = -\frac{1}{\beta}\ln P_i(X) \tag{7}$$

where $P_i(X)$ is the exact equilibrium probability distribution of X in the diabatic state i, $\beta = 1/k_BT$, and i is 1 or 2. $P_i(X)$ is found rigorously in the classical limit by integrating the delta function of X over phase space $d\Gamma$

$$P_i(X) = \frac{\int d\Gamma \delta(\Delta E - X)e^{-\beta E_i}}{\int d\Gamma e^{-\beta E_i}} \tag{8}$$

where E_i are the instantaneous energies of the system composed of the donor−acceptor complex and the solvent. In practice, this must be approximated through discrete functions via, for example, molecular dynamics (MD) or Monte Carlo (MC) simulations, where $P_i(X)$ is found by "binning" the reaction coordinate data.[16a,17b]

Both Marcus theory input parameters may be readily evaluated from simulation results:

$$\lambda = \frac{\langle X\rangle_1 - \langle X\rangle_2}{2} \tag{9}$$

$$\Delta F = \frac{\langle X\rangle_1 + \langle X\rangle_2}{2} \tag{10}$$

or through experimental data, as previously discussed. The consistency of the description also requires that the second moments are equal

$$\langle(\delta X)^2\rangle_1 = \langle(\delta X)^2\rangle_2 \tag{11}$$

This relation corresponds to the requirement of having equal spectral widths of emission and absorption lines originating from classical solvent fluctuations. The symbol $\langle ...\rangle_i$ above refers to the canonical average over the distribution function defined in eq 8.

The exact diabatic free energy curves are also exactly related by the expression[5,24]

$$F_2(X) = F_1(X) + X \tag{12}$$

This linear free energy relationship means that the two diabatic free energy surfaces must have the same local curvature at any given value of X. This concept is one of fundamental importance in ET reaction theory.[5]

III. Deviations from Marcus Theory

In the linear solvation approximation, the electronic diabatic energy in the donor and acceptor states, $I_i + C_iq$, depends linearly on q, the collective solvent mode driving ET. If the thermal fluctuations of q are described by Gaussian statistics, the free energy of creation of a nonequilibrium q in pure solvent is a quadratic function of q with the force constant κ: $(1/2)\kappa q^2$. The total energy of the donor acceptor complex and the solvent is then a bilinear function of q:

$$E_i = I_i + C_iq + \frac{1}{2}\kappa q^2 \tag{13}$$

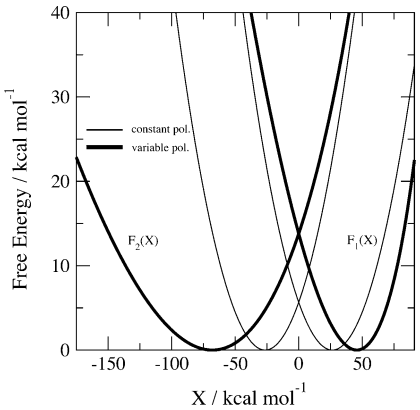

Figure 3. Example analytical ET free energy surfaces from ref 19. The fine curves correspond to a constant solute polarizability of 20 Å and follow Marcus theory curvature. The bold curves describe varying solute polarizability with $\alpha_1 = 20$ Å^3 and $\alpha_2 = 40$ Å^3 and demonstrate a clear deviation from Marcus theory curvature. In both systems, the solute permanent dipole moment varies from 0 to 15 D with the ET transition. The free energy curves are shifted vertically to the level of zero driving force to illustrate the asymmetry between the reactant and product states in the case when the polarizability changes with the transition.

where I_i is the intrinsic vacuum energy of diabatic state i. Because the force constant κ is equal for states 1 and 2, the energy gap $X = E_2 - E_1$ is a linear function of q. However, a more general expression for the system energy is given by[11b,25,26]

$$E_i = I_i + C_iq + \frac{1}{2}\kappa_i q^2 \tag{14}$$

Now the effective force constant is allowed to vary between states, hence the subscript on k_i. Using this expression for the electronic energies, the energy gap becomes bilinear in q if k_1 and k_2 differ.

If the collective force constant k_i driving ET does vary between states 1 and 2, significant departure from Marcus theory may be observed.[7a,b,e,16b−d,19,20] Physically, nonlinear coupling effects arise when the energy of polarization of the electronic density of the donor−acceptor complex by the nuclear subsystem is different in the initial and final states. The diabatic electronic energies E_i are then nonlinear functions of q.[20−22] When only the linear polarizability of the electronic density of the donor−acceptor complex is included, the solute−solvent coupling is bilinear in q, resulting in state-dependent k_i.[19] Matyushov and Voth demonstrated substantial variation in the curvature of the free energy functions in such systems[19,26] by deriving free energy surfaces analytically for a polarizable solute/solvent complex as modeled by Drude oscillators. They further considered a number of experimental systems where such variations may be observed.[20b,c]

Figure 3 shows an example of these analytical diabatic free energy surfaces. The fine curves (constant solute polarizability) display Marcus-like curvatures. The bold curves, corresponding to ET solute polarizability variation from 20 to 40 Å^3, display obvious variation in curvature and are anharmonic. In this case, the change in activation free energy upon treatment of solute polarizability variation is almost 20 kcal/mol, which translates

(25) (a) Nitzan, A.; Persson, B. J. *J. Chem. Phys.* **1985**, *83*, 5610. (b) Skinner, J. L.; Hsu, D. *J. Phys. Chem.* **1986**, *90*, 4931. (c) Berg, M. *J. Chem. Phys.* **1999**, *110*, 8577.
(26) Matyushov, D. V.; Voth, G. A. *J. Chem. Phys.* **2000**, *113*, 5413.

to orders of magnitude change in the reaction rate constant. Note that the apparent curvatures of the two diabatic curves in Figure 3 for the case of variable ET solute polarizability are very different, even though the local curvature is the same according to eq 12.[19]

IV. A New Three-Parameter Model

To accommodate a more realistic treatment of the diabatic free energy curves for ET systems (where variation in k_i is included), Matyushov and Voth developed a new three-parameter ET model,[26] and the reader is referred to the original paper for more details on the theoretical development. This model, called the "Q-model" due to the inclusion of quadratic coupling, incorporates a new parameter α, which quantifies the ET force constant variation. The fundamental expression for the diabatic free energy curves is

$$e^{-\beta E_i(X)+\beta F_{0i}} = \left(\frac{1}{1-e^{-\beta\lambda_i\alpha_i^2}}\right)\sqrt{\frac{\lambda_i|\alpha_i|^3}{|X-X_0|}}\, e^{-\beta(|\alpha_i||X-X_0|+\lambda_i\alpha_i^2)} I_1(2\beta\sqrt{|\alpha_i|^3|\lambda_i|X-X_0|}) \quad (15)$$

where $I_1(X)$ is the first-order modified Bessel function, and the relevant parameters are defined below. Under most conditions, this expression can be significantly simplified,[26] as will be shown later.

The Q-model is fully defined by three parameters. Equation 15 contains, however, five parameters: α_i, λ_i, and X_0. They are not independent due to the relations

$$\alpha_2 = \alpha_1 + 1 \quad (16)$$

$$\lambda_1\alpha_1^3 = \lambda_2\alpha_2^3 \quad (17)$$

which reduce the number of independent parameters to three. The reorganization energies λ_i are given in terms of the thermal fluctuations of the reaction coordinate around the free energy minima

$$\lambda_i = \frac{\beta\langle(X-\langle X\rangle_i)^2\rangle_i}{2} = \beta\hbar^2\langle\delta\omega^2\rangle_i/2 \quad (18)$$

The Q-model reorganization energies can be evaluated from either simulation data or data from spectroscopy experiments. Now the two reorganization energies can no longer be assumed to be equal, and eqs 1 and 2 are no longer valid. An alternate and more precise definition of the reorganization energies is through the absorption/emission bandwidths, or $\beta\hbar^2\langle\delta\omega^2\rangle_1/2$ and $\beta\hbar^2\langle\delta\omega^2\rangle_2/2$, also called the second spectral cumulants.

The three input parameters are λ_1, λ_2, and ΔF. The parameters in eq 15 can then be calculated from eqs 16, 17, and the relation

$$X_0 = \Delta F - \frac{\lambda_1\alpha_1^2}{\alpha_2} \quad (19)$$

This interdependence implicitly highlights the linear free energy relationship between the two ET surfaces. The parameters of the Q-model are also related to the first two spectral moments

$$\alpha_1 = \frac{(\hbar\Delta\omega_{st}+\lambda_2)}{\lambda_1-\lambda_2} \quad (20)$$

$$\Delta F = \hbar\omega_m - \frac{\lambda_1\alpha_1}{2\alpha_2^2} \quad (21)$$

where, for simulation data

$$\hbar\Delta\omega_{st} = \langle X\rangle_1 - \langle X\rangle_2 \quad (22)$$

$$\hbar\omega_m = \frac{\langle X\rangle_1 + \langle X\rangle_2}{2} \quad (23)$$

Equation 21 indicates that the mean spectral energy and the driving force are unequal in the Q-model. The difference between these two parameters which can be measured independently is represented in terms of spectroscopic observables as follows

$$\hbar\omega_m - \Delta F = \frac{\lambda_1(\lambda_1-\lambda_2)(\hbar\Delta\omega_{st}+\lambda_2)}{2(\hbar\Delta\omega_{st}+\lambda_1)^2} \quad (24)$$

For most reaction coordinate values ($2\beta\sqrt{|\alpha_i|^3\lambda_i|X-X_0|} \gg 1$), the Q-model free energy equation reduces to a simpler form

$$F_i(X) = F_{0i} + (\sqrt{|\alpha_i||X-X_0|} - |\alpha_i|\sqrt{\lambda_i})^2 \quad (25)$$

If $|\alpha_i| \gg 1$, $\lambda_1 \simeq \lambda_2 = \lambda$, and eq 25 reduces to

$$F_i(X) = F_{0i} + \frac{(X-\Delta F \mp \lambda)^2}{4\lambda} \quad (26)$$

which is equivalent to the Marcus expressions (eqs 5 and 6). In the limit that $|X-X_0| \gg \lambda_i|\alpha_i|$, the Q-model formula becomes

$$F_i(X) = F_{0i} + |\alpha_i||X - \Delta F + \lambda_1\frac{\alpha_1^2}{\alpha_2}| \quad (27)$$

that is, the dependence on the reaction coordinate becomes linear. Because the magnitude $X = 0$ defines the activated state, the limiting behavior of eq 27 yields the linear energy gap law.[10] Example free energy surfaces calculated from the three-parameter model equations are shown in Figure 4. The way in which the parameters in the Q-model can be defined from experimental data is defined in ref 26, but this is not the main focus of the present paper.

V. Simulations of Polarizable Solute/Solvent Systems

The primary goal of the present paper is to test the accuracy of the new three-parameter ET model for realistic systems. Molecular dynamics simulations were therefore conducted in a condensed-phase system with both a polarizable ET solute and a polarizable solvent.

(A) Simulation Details. All simulations were performed with the DL_POLY 2 molecular dynamics simulation package.[27] The DL_POLY FORTRAN code was modified to include sampling

(27) Smith, W.; Forester, T. R. 1996 CCLRC Daresbury Laboratory, Daresbury, Warrington, U.K.

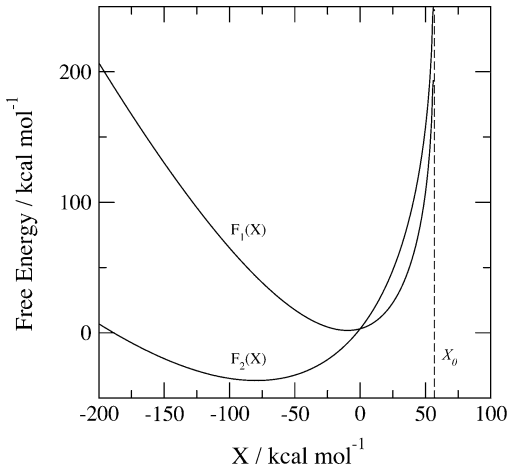

Figure 4. Example of Q-model free energy surfaces. The analytical Q-model solution results in a discontinuity at X_0. ET free energies exist in the region to the right of X_0 when $\alpha_1 > 0$ ($F_i(X) \rightarrow \infty$ for $X < X_0$), and the region to the left of X_0 when $\alpha_1 < -1$ ($F_i(X) \rightarrow \infty$ for $X > X_0$).

of the reaction coordinate. All simulations had a canonical ensemble via Nose−Hoover thermostating[28] at a temperature of 300 K, and the smooth particle mesh Ewald method[29] was used to evaluate the electrostatic forces.

The shell model[30] was used to model the polarizability of both the solute and the solvent molecules. In this model, outer shell electrons are represented by a point charge connected to the core atom via a harmonic spring. The shell particle is given a very small mass so that thermal energy transferred to the nuclei from shell motion will be minimal.[30c] To remain on an adiabatic potential energy surface, the shell particles should be at equilibrium at each simulation time step. This effect is approximated by using a small shell mass and a short time step.[30c] The harmonic spring is atom centered; on average, the shell position will be the same as the core atom position, and the two form one unit. The shell potential energy is given by

$$E_{sh} = \frac{1}{2}kr^2 \tag{28}$$

For a molecule containing n shell particles each of equal charge q_{sh} and force constant k, the polarizability is given by

$$\alpha = \frac{nq_{sh}^2}{k} \tag{29}$$

In all simulations, water was used as the solvent. The solvent molecules consist of one shell particle centered on the oxygen atom. The O−H bond was constrained with SHAKE.[31] The H−O−H angle was constrained by introducing an H−H intramolecular bond, also held rigid with SHAKE.

(B) Umbrella Sampling. Often the horizontal energy gap between the diabatic free energy surfaces in an ET system is on the order of tens or hundreds of kcal/mol. Molecular dynamics must be extended to sample over such ranges within a realistic amount of computer time. A useful method to accomplish this is umbrella sampling.[32a] In umbrella sampling, a biasing potential is added to the system Hamiltonian to force the system into states and configurations that are normally visited very infrequently. Two independent types of umbrella sampling were employed in this study, the free energy perturbation (FEP) method and the harmonic umbrella potential (HUP) method. In FEP, the reactant Hamiltonian is transformed into the product Hamiltonian through a linear combination:[16a,17a,32b]

$$H_{umb} = (1 - \lambda_{umb})H_1 + \lambda_{umb}H_2 = H_1 + \lambda_{umb}(\Delta E) \tag{30}$$

and the force on each atom is

$$f_{umb}(x,y,z) = f_1(x,y,z) + \lambda_{umb}(f_2(x,y,z) - f_1(x,y,z)) \tag{31}$$

Typically a series of λ_{umb} values is chosen, and a separate simulation is performed for each λ_{umb}. Each simulation is termed a "window".

In the HUP method, the biasing potential is a harmonic function of the reaction coordinate,[17d] and the Hamiltonian becomes

$$H_{umb} = H + \frac{1}{2}k(\Delta E - \Delta e_0)^2 \tag{32}$$

where k is an effective force constant, and Δe_0 is the point along the reaction coordinate where sampling is constrained to occur. The force on each atom is then

$$f_{umb}(x,y,z) = f_i(x,y,z) - k(\Delta E - \Delta e_0) \times (f_1(x,y,z) - f_2(x,y,z)) \tag{33}$$

where i is 1 or 2 depending on which potential surface the system is on. Again, several windows are used, each with a different value for Δe_0.

The weighted histogram analysis method (WHAM)[33] provides an algorithm to produce a single converged free energy curve for a series of umbrella sampling windows, regardless of the type of umbrella potential used. This method was used for all simulation results.

(C) Polarizable Solute Simulations. The solute contains six carbon and six hydrogen atoms in a hexagonal ring geometry, with a shell particle attached to a dummy atom centered within the ring. The parameters used for the solute are given in Table 1, and those of the solvent are given in Table 2. The solute has dipole moments of 3.6 and 9.8 D for the initial and final states, with corresponding polarizabilities of 4.43 and 8.86 Å^3. It must be emphasized that these simulations were not intended to model any real property of benzene. The solute in this study was chosen only to have a realistic change in dipole moment and electronic polarizability.

Twenty-one FEP umbrella windows were used, and data were collected for ~50 ps in each window, at a time step of 0.4 fs. In the HUP simulations, 21 windows were used for the initial state, and 16 were used for the final state. Data were collected for ~50 ps in each window, at a time step of 0.4 fs. The simulation results were compared with the Q-model by using

(28) Hoover, W. G. *Phys. Rev. A* **1985**, *31*, 1695.
(29) Essmann, U.; Perera, L.; Berkowitz, M. L.; Darden, T.; Lee, H.; Pedersen, L. G. *J. Chem. Phys.* **1995**, *103*, 8577.
(30) (a) Dick, B. G.; Overhauser, A. W. *Phys. Rev.* **1958**, *112*, 90. (b) Fincham, D.; Mitchell, P. J. *J. Phys.: Condens. Matter* **1993**, *5*, 1031. (c) van Maaren, P. J.; van der Spoel, D. *J. Phys. Chem. B* **2001**, *105*, 2618. (d) Rick, S. W.; Stuart, S. J. In *Rev. Comput. Chem.*; Lipkowitz, K. B., Boyd, D. B., Eds.; Wiley-VCH: Hoboken, New Jersey, 2002; Vol. 18.
(31) Allen, M. P.; Tildesley, D. J. *Computer Simulations of Liquids*; Oxford: Clarendon Press, 1989.
(32) (a) Torrie, G. M.; Valleau, J. P. *J. Comput. Phys.* **1977**, *23*, 187. (b) DeBolt, S. E.; Pearlman, D. A.; Kollman, P. A. *J. Comput. Chem.* **1994**, *15*, 351.
(33) Kumar, S.; Bouzida, D.; Swendsen, R. H.; Kollman, P. A.; Rosenberg, J. M. *J. Comput. Chem.* **1992**, *13*, 1011.

Table 1. Solute Model Parameters[a]

parameter	value	parameter	value	parameter	value
r_{C-C}	1.4	M_C	11.98	M_H	1.0
M_{Du}	0.1	M_{SH}	0.1	$\epsilon^{LJ}_{C-O_{SH}}$	0.1955
ϵ^{LJ}_{C-O}	0.0955	$\epsilon^{LJ}_{C_{SH}-O_{SH}}$	0.36854	$\epsilon^{LJ}_{C_{SH}-O}$	0.21059
$\sigma^{LJ}_{C-O_{SH}}$	3.1861	σ^{LJ}_{C-O}	3.1861	$\sigma^{LJ}_{C_{SH}-O_{SH}}$	3.1861
$\sigma^{LJ}_{C_{SH}-O}$	3.1861				

	state 1	state 2		state 1	state 2		state 1	state 2
q_{C1}	0.400	0.634	q_{C4}	0.134	−0.100	q_H	0.400	0.400
q_{C2}	0.400	0.633	q_{C5}	0.133	−0.100	q_{SH}	−4.0	−4.0
q_{C3}	0.400	0.633	q_{C6}	0.133	−0.100	k_{SH}	1200.0	600.0

[a] The masses are in amu, the bond lengths are in Å, the energies are in kcal mol^{-1}, the force constants are in kcal mol^{-1} Å^{-2}, and the charges are in electron charge units.

Table 2. Water Solvent Parameters[a]

parameter	value	parameter	value	parameter	value
r_{OH}	0.9572	r_{HH}	1.5136	M_O	15.9
M_H	1.0	M_{SH}	0.1	q_0	1.2
q_H	0.4	q_{SH}	−2.0	k_{SH}	885.0
$\epsilon^{LJ}_{O-O_{SH}}$	0.21059	ϵ^{LJ}_{O-O}	0.05265	$\epsilon^{LJ}_{O_{SH}-O_{SH}}$	0.36854
$\sigma^{LJ}_{O-O_{SH}}$	3.1650	σ^{LJ}_{O-O}	3.1650	$\sigma^{LJ}_{O_{SH}-O_{SH}}$	3.1650

[a] The units are the same as those in Table 1.

the following prescription: First, the average energies for each diabatic state, $\langle X\rangle_1$ and $\langle X\rangle_2$, were found by averaging over the simulation data from the $\lambda_{umb} = 0.0$ and $\lambda_{umb} = 1.0$ windows. The Stokes shift and mean energy were then calculated through eqs 22 and 23, respectively.

The prescription for matching the analytical curves to data calls[26] for calculating λ_1 and λ_2 with eq 18, and then using the two calculated parameters together in the Q-model equations (e.g., eqs 17, 20, etc.). This may produce an incongruous fit, because the calculation of reorganization energies through eq 18 can be inaccurate, especially when the two reorganization energies differ substantially. The consistency criterion of eq 17 was used iteratively to improve the fit quality. The parameter λ_1 was first calculated via eq 18 by averaging over the data from the $\lambda_{umb} = 0.0$ simulation. The parameter λ_2 was likewise found using the $\lambda_{umb} = 1.0$ data. Through eqs 16, 17, and 20, a polynomial expression can be obtained for α_1 in terms of λ_2:

$$(2\lambda_2 - \hbar\Delta\omega_{st})\alpha_1^2 + 3\lambda_2\alpha_1 + \lambda_2 = 0 \qquad (34)$$

Only one of the solutions to this equation is physically significant. Using this α_1, the λ_2 from simulation data, and eq 17, we calculated a second λ_1. A more accurate λ_1 is then found by taking the average of the two produced λ_1 values.

Again, through eqs 16, 17, and 20, a polynomial expression can be obtained for α_1, but this time in terms of λ_1:

$$(\hbar\Delta\omega_{st} - 2\lambda_1)\alpha_1^3 + (3\hbar\Delta\omega_{st} - 3\lambda_1)\alpha_1^2 + (3\hbar\Delta\omega_{st} - \lambda_1)\alpha_1 + \hbar\Delta\omega_{st} = 0 \qquad (35)$$

As with eq 34, only one of the solutions to this equation will be physically significant. By substituting the averaged λ_1 in eq 35, we found that the resulting α_1 will have higher accuracy. The parameter α_2 was then calculated from eq 16, and λ_2 was calculated from eq 17. The remaining parameters were then found through eqs 19 and 21. By applying the Q-model in this manner, we assured that none of the crucial relationships (eqs 12, 16, 17, 19, 21) are violated. The simplified Q-model expression, eq 25, was then used for the fitting. The results for the FEP and HUP simulations are shown in Figures 5 and 6, respectively.

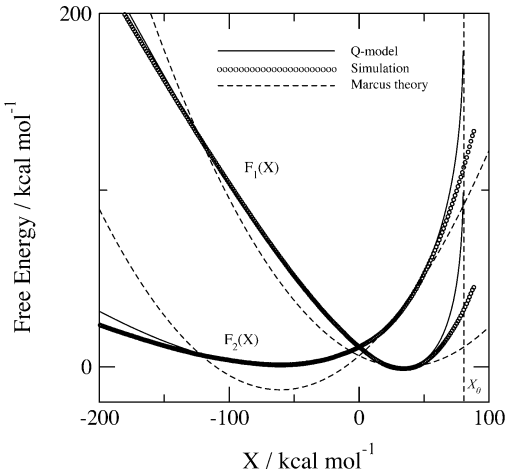

Figure 5. FEP simulation (circles), Q-model (bold lines), and Marcus theory (dashed lines) surfaces for the system with varying solute polarizability. The Marcus theory result (calculated from eqs 5 and 6) assumes a constant solute polarizability. Each simulation curve has 300 data points (bins).

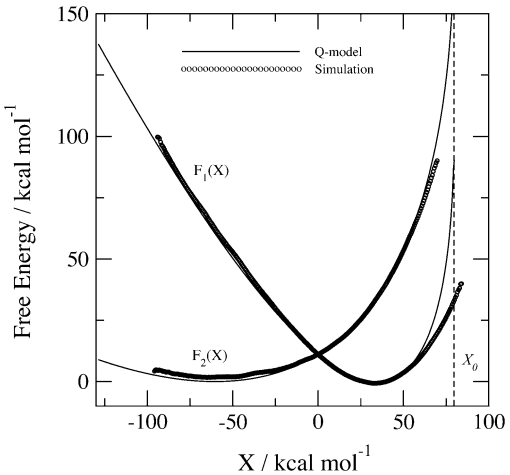

Figure 6. HUP simulation results and Q-model surfaces for the benzene system with varying solute polarizability. Each simulation curve has 300 data points (bins).

The Q-model fits the simulation curves very well in the important regions along the reaction coordinate (between the minima). The Q-model curves begin to deviate from the simulation curves far from the state 2 minimum. Toward the reactant side away from the state 1 minimum, the simulation curves develop a steep ascent, but not the discontinuous jump to infinity predicted by the Q-model. Most importantly, however, these results illustrate for the first time the size of the possible deviations from the standard Marcus theory prediction when the change in solute electronic polarizability is treated in a realistic system. The new Q-model, implemented as outlined in detail in the beginning of this section, gives a good description of the large deviations from the traditional theory.

VI. Conclusions

Two types of experiments are commonly used to describe the thermodynamics and dynamics of electronic transitions in liquid and solid solvents: rates of thermally activated reactions

(ET kinetics) and optical spectroscopy. These two types of measurements are essentially complementary, the former measuring the tails of the system distribution $P_i(X)$ (eq 8) over the reaction coordinate (activated transitions), and the latter measuring the distribution close to the reactant and product minima. Both types of measurements provide evidence that the traditional Marcus picture requires modification. ET kinetics show asymmetry between CS and CR energy gap laws, while optical spectroscopy data often show asymmetry between absorption and emission optical bands. (That is, the absorption and emission bands may be asymmetric due to the vibronic progressions of each, but the traditional theory predicts a perfect mirror symmetry between the two bands, and this is often not the case.)

The present study is a step toward the development of a new conceptual framework allowing a consistent explanation of seemingly unlinked measurements from ET kinetics[7−10] and steady-state[12] and time-resolved[13] spectroscopy. The analytical development preceding this paper[19,20,26,34] predicts marked deviations from the picture of two equal-curvature parabolas when the electronic subsystem of the donor−acceptor complex is coupled nonlinearly to the nuclear subsystem. The key distinction of the new concept from the Marcus picture is the notion that an electronic transition results not only in a change of the distribution of charge in the donor−acceptor complex, but also in a change of the polarization energy of the donor−acceptor complex by the system (solute and/or solvent) nuclei. This polarization energy may include linear and higher order polarizabilities. The present study focuses on the effect of linear solute polarizability that varies with the electronic transition.

The polarization energy of the solute depends quadratically on the electric field of the solvent when the expansion in the field strength is truncated at the linear polarizability term.[35] The charge distribution of the solute is linearly coupled to the solvent electric field in the dipolar approximation. The combination of these two factors leads to the analytical Q-model producing nonparabolic free energy surfaces of ET.[19,26] The qualitative results of the model explain the principal experimental observations conflicting with the Marcus picture: the asymmetry between the CS and CR energy gap curves and the asymmetry between the absorption and emission band-shapes (Figures 5−7). In addition, the Q-model predicts a linear energy gap law. The latter is often observed,[10] but is traditionally explained within vibronic models.[11]

This paper shows that the results of the Q-model coincide very closely with free energy surfaces obtained from large-scale umbrella sampling MD runs on a realistic liquid-state system. The simulations were performed by using shell models for both the solute and the solvent.[30] In this setup, the polarization energy of the solute is quadratic in the solvent electric field, while the solute−solvent interaction includes both dipolar and higher-order multipolar interaction terms. The latter aspect may be responsible for deviations between the analytical theory and MD simulations in the region of reaction coordinates close to the boundary X_0 in the Q-model calculations (Figures 5 and 6). The analytical Q-model includes only the dipolar component of the solvent field. With quadratic solute−solvent coupling, there is no analytical solution for the dipolar solvent field that can create

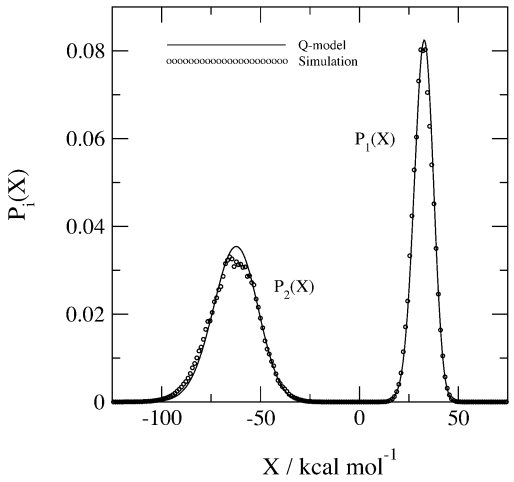

Figure 7. Equilibrium distributions in the reactant and product states from FEP simulations and the Q-model.

the resonance between the donor and acceptor electronic levels necessary for electron tunneling when the energy gap exceeds some critical value X_0. This result limits the range of the energy gap fluctuations to a one-sided band. In actual simulations, fluctuations of nondipolar polarization of the solvent, as well as coupling of higher solute multipoles to gradients of the solvent field, can offset the fluctuation boundary or eliminate it completely. This intriguing problem warrants further studies. It should be noted that a very asymmetric energy gap distribution with a cutoff similar to the prediction of the Q-model has been recently observed in simulations of naphthalene in acetonitrile by Cichos et al.[36]

The Q-model can be fully parametrized by measurements of the first two spectral moments of the absorption and emission lines. In computer simulations, the spectral moments are replaced by the moments of the reaction coordinate calculated from the data from the windows of the reactant and product minima. These moments were used in Figures 5 and 6 to construct analytical curves. Comparing the analytical results to direct MD simulations in this way displays the predictive power of the Q-model. Figure 7 shows the corresponding equilibrium distributions in the reactant and product states. They correspond to the solvent-induced component of inhomogeneously broadened line-shapes in optical experiments. The complete vibronic envelope in a condensed-phase solvent can be obtained by convoluting the distributions $P_i(X)$ shown in Figure 7 with gas-phase vibronic band-shapes.[20b,c] The inverse process of deconvolution of experimental optical lines leads to a new formulation of the band-shape analysis of steady-state[19,20b,c] and time-resolved[34] CT optical bands. Figures 5 and 6 indicate that both the energy barrier and the free energy gap obtained from spectral moments and/or the band-shape analysis of optical lines according to the Marcus model can be significantly inaccurate. The reason for the distinction in the driving force is that the latter calculated according to the Q-model (eq 21) is not equal to the mean optical transition energy as predicted by the Marcus model (eq 2). This distinction may be used for a direct experimental verification of the Q-model because the difference of the spectral mean energy and the thermodynamic driving force is predicted to be related to a combination of the first and second spectral moment according to eq 24. A general conclu-

(34) Matyushov, D. V. *J. Chem. Phys.* **2001**, *115*, 8933.
(35) Liptay, W. In *Modern Quantum Chemistry, Part II: Interactions*; Sinanoğlu, O., Ed.; Academic Press: New York, 1965.
(36) Cichos, F.; Brown, R.; Bopp, Ph. A. *J. Chem. Phys.* **2001**, *114*, 6824.

sion arising from the present work is that the standard theory of ET free energies requires significant modification when nonlinear solute−solvent coupling is present, for example, when the electronic polarizability varies significantly between the reactant and product ET states.

Acknowledgment. This work was supported by the U.S. Department of Energy Solar Photochemistry Program of the Office of Basic Energy Sciences.

JA029595J